Experiments on negative and positive magnetoviscosity in an alternating magnetic field

A. Zeuner, R. Richter,* and I. Rehberg
Institut für Experimentelle Physik, Abteilung Nichtlineare Phänomene, Otto-von-Guericke Universität, Postfach 4120, D-39016 Magdeburg, Germany
(Received 19 May 1998)

Recently it has been predicted and shown experimentally that the viscosity of a magnetic fluid flowing through a capillary pipe (Hagen-Poiseuille flow) can be reduced under the influence of an alternating, linearly polarized magnetic field. We present experimental results of the amplitude and frequency dependence of this ''negative viscosity effect.'' Experimental data are quantitatively compared with results we have obtained by numeric integration of a prevailing model. [S1063-651X(98)12711-3]

PACS number(s): 83.85.Jn, 47.15.−x, 75.50.Mm

I. INTRODUCTION

When at the beginning of this century Einstein estimated the viscosity for a suspension of hard spheres [1] he did not consider the possibility that the spheres could as well be made from magnetic material. Indeed such complex and man-made magnetic fluids were not available before the 1960s. They are colloidal dispersions of magnetic nanoparticles in a liquid carrier [2]. In order to prevent the particles from sticking together a molecular coating by surfactants is applied. Since the properties and location of these fluids can easily be influenced by an external magnetic field, they have recently attracted much scientific and technological interest [3–5]. Already existing applications include magnetic fluid rotary seals which can be found in 60% of the PC's hard drives, sink-float separation of minerals, diagnostics in medicine, the magnetic clutch, and tunable dampers.

Some of the applications utilize the fact that the viscosity of the magnetic fluid increases in a stationary magnetic field. This was already discovered in 1969 by McTague [6] in an experiment investigating magnetic fluid in a Hagen-Poiseuille flow. The external magnetic field hinders the free rotation of the magnetic nanoparticles and thus increases the viscosity of the flow. A theoretical treatment giving the viscosity of dilute suspensions and accounting for the Brownian rotational motion of the particles was presented by Shliomis in 1972 [7] and later modified in a review article in 1988 [8]. For the reduced viscosity he obtained

$$\eta_r = \frac{\Delta\eta}{\eta} = \frac{3}{2}\phi_h \frac{\xi L^2}{\xi - L}\sin^2\beta. \tag{1}$$

Here ϕ_h denotes the volume fraction of the hydrodynamic effective volume of the particles, i.e., the volume of the magnetic particles with their surfactants in the fluid. The Langevin parameter $\xi = mH/kT$ characterizes the ratio between the energy of the magnetic moment m of the particle in the magnetic field H and its thermal energy kT. The Langevin function L is given by $L(\xi) = \coth(\xi) - 1/\xi$. The angle between the direction of the field H and the local angular velocity of the particle is measured by β.

Later, in 1994, Shliomis and Morozov [9] investigated the additional viscosity generated in a flow with vorticity due to an alternating, linearly polarized magnetic field. They postulated a negative viscosity contribution ($\Delta\eta < 0$) for a certain range of the frequency and field strength of the applied magnetic field. This ''negative viscosity effect'' can be understood as a transfer of energy from the magnetic field into rotational motion of the particles. They act like nanosize motors and actively reduce the friction between neighboring fluid layers.

The performance of these nanomotors depends on the mechanisms by which they respond to a change of the external magnetic field. These mechanisms are the Brownian relaxation and the Néel relaxation. In the case of Brownian relaxation, a particle rotates together with its magnetic moment which is fixed relative to the crystal axis of the particle. This mechanism is characterized by a rotational diffusion time τ_B of hydrodynamical origin which is given by

$$\tau_B = \frac{3\eta_0 V_h}{kT}. \tag{2}$$

Here η_0 is the viscosity of the carrier liquid, V_h the hydrodynamic effective volume of the particle, and kT the thermal energy. The second mechanism is the rotation of the magnetic moment of the particle relative to the crystal axis of the particle, the Néel relaxation. Its characteristic relaxation time τ_N is expected to be much larger than the Brownian relaxation time for our ferrofluid [2]. It is obvious that only the first mechanism contributes to the negative viscosity effect whereas the Néel relaxation in this context can be seen as a parasitic effect.

The negative viscosity effect has recently been detected by Bacri *et al.* [10] by means of a colloidal suspension of Co-ferrite ($Co\,Fe_2O_4$) particles of 10 nm. We use a different material, namely magnetite (Fe_3O_4), and present measurements for the amplitude and frequency dependence of the negative viscosity effect, which are quantitatively compared with the theoretical predictions.

Our paper is organized as follows. After introducing the experimental setup in Sec. II, Sec. III describes the experimental findings. In Sec. IV we quantitatively compare the

*Author to whom correspondence should be addressed. FAX: ++391-6718108. Electronic address: reinhard.richter@physik.uni-magdeburg.de

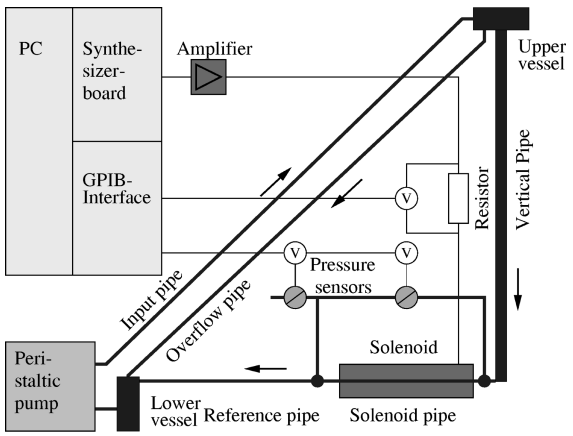

FIG. 1. Scheme of the experimental setup.

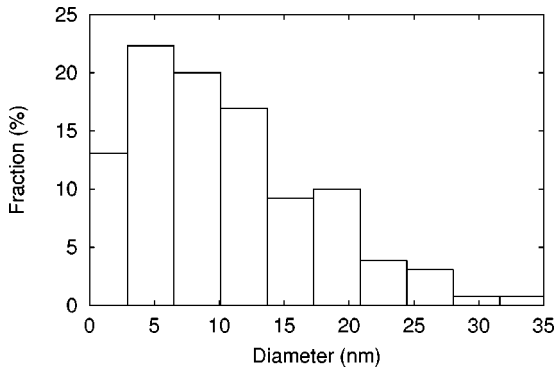

FIG. 2. Distribution of the particle size as measured with the transmission electron microscope.

results regarding the negative viscosity effect with the theoretical description given in Refs. [9,10]. The conclusion is presented in Sec. V.

II. EXPERIMENTAL SETUP

We established a continuous flow of magnetic fluid in a closed system of pipes in order to favor an automated data acquisition, suitable to scan the extended parameter space. Figure 1 depicts the experimental setup. An upper vessel is connected in series with a vertical pipe and two capillary pipes of diameter 1 mm to a lower vessel. The latter is used as a reservoir. A peristaltic pump (Watson-Marlow, type: WM 505–UR/220) and an overflow maintain a constant fluid level in the upper vessel thus establishing a constant pressure drop across the two capillary pipes. One of the capillaries is mounted in the center of a solenoid which is cooled by water. The solenoid is connected to a power amplifier (VC 2400 of HK Audio) which is driven by a synthesizer board (WSB-100 of Quatech Inc.) mounted in a 486-PC. A digital multimeter (Prema DMM 6001) captures the voltage drop across the load resistors in order to control the amplitude of the alternating field. Two electric pressure sensors measure the pressure drop across the capillary pipe in the solenoid (Δp_{sol}) and across the reference pipe (Δp_{ref}). Their voltage is simultaneously recorded by two multimeters (Prema DMM 6001) connected via a GPIB-Interface to the computer. Via the Hagen-Poiseuille formula for the mass flow rate one obtains for the ratio of viscosities with (η_{mag}) and without (η) a magnetic field the expression

$$\frac{\eta_{\mathrm{mag}}}{\eta}=\frac{\Delta p_{\mathrm{sol,mag}}}{\Delta p_{\mathrm{sol}}}\,\frac{\Delta p_{\mathrm{ref}}}{\Delta p_{\mathrm{ref,mag}}}, \tag{3}$$

where $\Delta p_{\mathrm{sol,mag}}$ is the pressure difference across the capillary pipe in the solenoid with a magnetic field, and $\Delta p_{\mathrm{ref,mag}}$ is the pressure difference across the reference pipe in the presence of a magnetic field. For the reduced viscosity η_r then follows,

$$\eta_r=\frac{\eta_{\mathrm{mag}}-\eta}{\eta}=\frac{\eta_{\mathrm{mag}}}{\eta}-1. \tag{4}$$

An advantage of the experimental arrangement is its robustness to fluctuations in the temperature because only the ratio of the viscosities is determined. Due to the short settling time of the flow the pressure drop with and without a magnetic field can be measured within 4 s.

The pipe system is filled with the magnetic fluid (MF) under investigation. We have selected a water based dispersion of magnetite particles, namely, EMG 705 available from Ferrofluidics Corporation. Its properties at room temperature ($T=295.2$ K) are density $\rho_{MF}=1190\ \mathrm{kg\,m^{-3}}$, surface tension $\sigma=4.75\times10^{-2}\ \mathrm{kg\,s^{-2}}$, initial magnetic permeability $\mu=1.56$, magnetic saturation $M_S=0.02$ T, and dynamic viscosity $\eta=6\times10^{-3}\ \mathrm{Ns\,m^{-2}}$ according to the manufacturer. The anisotropy constant of magnetite is given to be $K=8\times10^{4}\ \mathrm{J\,m^{-3}}$ [2], and the domain magnetization is expected to be $M_d=0.56$ T [2].

The distribution of the diameter of the magnetite particles is displayed in Fig. 2. It has been estimated from a set of 130 samples measured by means of a transmission electron microscope (Philips CM200) and an object recognition software (AnalySIS 2.11). For the arithmetic mean diameter we obtain $\bar{d}=12.2$ nm. With the diameters of the particles we calculate the average magnetic dipole moment of the particles to be $m=1.1\times10^{-24}$ V s m by means of the identity $m=M_dV_{\mathrm{core}}$, where $V_{\mathrm{core}}=(1/N)\Sigma_i^N(\pi/6)d_i^3$ denotes the averaged volume of the bare particles, when assuming spherical particles. The value of $V_{\mathrm{core}}=2.05\times10^{-24}\ \mathrm{m^3}$ is two times larger than the value of $9.5\times10^{-25}\ \mathrm{m^3}$ for the volume of the particle which would be obtained from the mean diameter of the particles.

Using Eq. (2), and taking the averaged volume of the particles as the hydrodynamic effective volume, one gets $\tau_{B,\mathrm{core}}=1.5\times10^{-6}$ s. Note that this number is only a lower bound of the Brownian relaxation time, because the hydrodynamic effective volume is believed to be determined by the surfactant layer around the particles. In addition, the agglomeration of particles would also tend to increase this number.

In order to determine the relaxation times experimentally, we have measured the complex magnetic ac susceptibility following the method described in Ref. [11], which yields an effective relaxation time $\tau_{\mathrm{eff}}=9.4\times10^{-5}$ s. This effective relaxation time is determined by a combination of the Brownian and Néel relaxation times. An estimate of the effective relaxation time is given by [12]

$$\tau_{\mathrm{eff}}=\frac{\tau_N\tau_B}{\tau_N+\tau_B}. \tag{5}$$

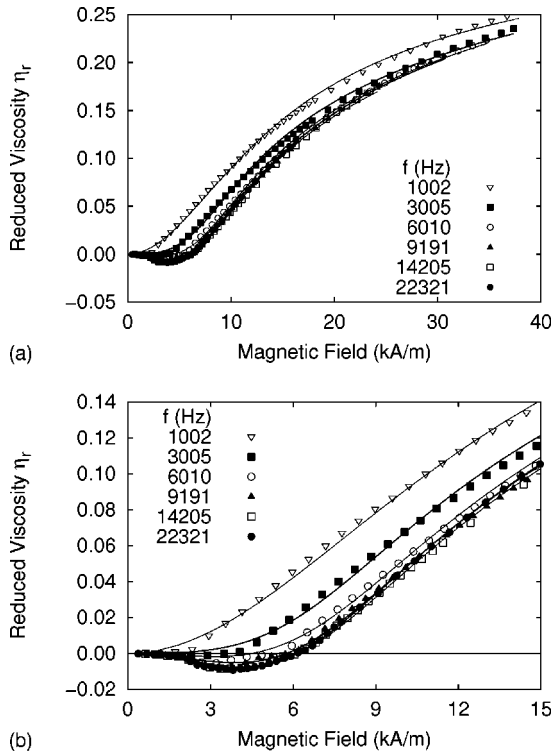

FIG. 3. (a) Reduced viscosity as a function of the magnetic field for six different frequencies of the magnetic field; (b) enlargement of (a).

Using this equation we estimate the Brownian relaxation time from

$$\tau_B = \frac{\tau_N \tau_{\mathrm{eff}}}{\tau_N - \tau_{\mathrm{eff}}} \tag{6}$$

to be $\tau_{B,\mathrm{sus}} = 9.4 \times 10^{-5}$ s, where a value of about 1 s has been used as an estimate of τ_N [2].

III. EXPERIMENTAL RESULTS

For a set of 14 different values of the driving frequency the reduced viscosity η_r has been measured in dependence on the amplitude of the alternating magnetic field. Figure 3(a) gives six representative curves. Each point has been obtained from an average of ten independent measurements of the reduced viscosity. All curves show a continuous increase of η_r for higher values of the amplitude of the magnetic field. In order to unveil subtleties in the vicinity of the origin we focus our attention to the enlargement given in Fig. 3(b). The curves for 1002 Hz and 3005 Hz continue to show a monotonous increase starting from a plateau at $\eta_r = 0$. However, for higher frequencies we clearly observe a negative viscosity contribution, which becomes more prominent with increasing values of the driving frequency. At the same time the center of the minimum is shifted to higher values of the amplitude of the magnetic field. For 22 321 Hz we observe a reduction of the magnetoviscosity of about 1%. Another remarkable feature is the similar shape of the curves of the reduced viscosity once $\eta_r = 0$ is surpassed.

IV. COMPARISON WITH THEORY

In the following we perform a comparison of our experimental data with the predictions of a theoretical model recently proposed [9]. We start with the integration of a set of ordinary differential equations given in Ref. [10] which are based on that model. Subsequently we fit this model to the experimental data. In the third part we focus on the qualitative features that experiment and model have in common.

A. The model equations

The ordinary differential equations suggested in [10] for a flow of small vorticity are

$$\tau_B \frac{d\xi_e}{dt} = -\left(\frac{d \ln L_e}{d\xi_e}\right)^{-1}\left(1 - \frac{\xi_0}{\xi_e}\cos(\omega t)\right), \tag{7}$$

$$\tau_B \frac{dF}{dt} = 1 - \frac{1}{2}\left(\frac{1}{L_e} - \frac{1}{\xi_e}\right)\xi_0 F \cos(\omega t). \tag{8}$$

Here $\xi_e = mH/kT$ denotes the effective field, and ξ_0 is defined over the amplitude H_0 of the magnetic field. Solving this equation up to relaxation and averaging the relaxed solution over one period of the external magnetic field $\xi = \xi_0 \cos(\omega t)$ the function

$$g(\omega\tau_B, \xi_0) = \frac{1}{2}\xi_0 \overline{\cos(\omega t) L(\xi_e) F(\xi_e)} \tag{9}$$

was estimated. It determines the reduced viscosity η_r by means of the equation

$$\eta_r(\omega\tau_B, \xi_0) = \frac{3}{2}\phi g(\omega\tau_B, \xi_0). \tag{10}$$

However, solving Eq. (8) becomes complicated, because the poles of F at $\xi_e = 0$ have to be taken into account. In order to overcome these problems we prefer to solve a mathematically equivalent system, consisting of Eq. (7) and the equation for the derivative of the product of L and F:

$$A(\xi_e) = L(\xi_e) F(\xi_e). \tag{11}$$

From Eqs. (7) and (8) we obtain

$$\tau_B \frac{dA}{dt} = L_e + A\left(\xi_0 \frac{3L_e - \xi_e}{2\xi_e L_e}\cos(\omega t) - 1\right). \tag{12}$$

Now the function $g(\omega\tau_B, \xi_0)$ is determined by

$$g(\omega\tau_B, \xi_0) = \frac{1}{2}\xi_0 \overline{\cos(\omega t) A(\xi_e)}. \tag{13}$$

We solve the systems of Eqs. (7) and (12) using an Adams-Bashforth-Moulton predictor-corrector method of fourth order up to relaxation and calculate the integral over one period as given by Eq. (13). The initial conditions are $\xi_e(0) = \xi_0$ and $A(0) \approx 0$, similar to those in Ref. [10]. The required starting values for this method are calculated using the classical Runge-Kutta method of fourth order. Note that in comparison to the well known Runge-Kutta formulas of

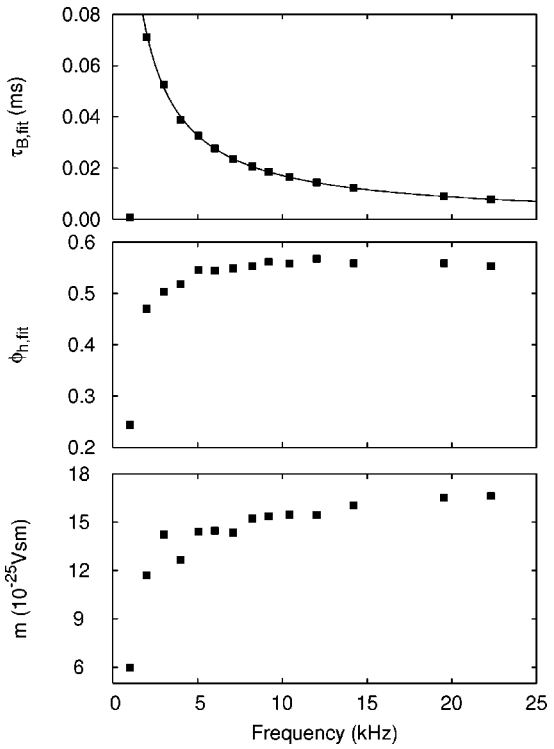

FIG. 4. Results of the fitting procedure with Eq. (10). The solid line is the fit according to Eq. (16).

the same order the applied method requires only half the number of evaluations of the complicated derivatives.

B. Quantitative comparison

Next we fit Eq. (10) to our experimental data. The solid lines in Figs. 3(a) and 3(b) display the curves obtained by a fit utilizing Marquart's method [13]. The fitting parameters, namely, the magnetic dipole moment m, the volume fraction ϕ, and the Brownian relaxation time τ_B, are shown as a function of the driving frequency in Fig. 4 bottom to top, respectively.

The Brownian relaxation time obtained from the fitting procedure $\tau_{B,\mathrm{fit}}$ decays with the driving frequency. The value obtained for 1002 Hz seems to be special. The explanation is that $\tau_{B,\mathrm{fit}}$ cannot be determined for very low frequencies, which is caused by the fact that there is no phase shift between the field and the orientation of the magnetic dipoles in this limit. Precisely speaking, this means that

$$\lim_{\omega\to 0}\frac{\partial g}{\partial \tau_B}=0. \tag{14}$$

The fitting procedure gives a value of about 8×10^{-7} s at this frequency. It is obvious that this value has no physical meaning, it must be considered as an artifact of the fitting procedure for low frequencies. Note that the values for the volume fraction and the magnetic dipole moment are not influenced by this singularity. A fit to the temporal average of Eq. (1),

$$g(\omega\tau_B\to 0,\xi_0)=\frac{1}{T}\int_0^T\frac{\xi(t)L^2(\xi(t))}{\xi(t)-L(\xi(t))}dt, \tag{15}$$

with $\xi(t)=\xi_0\cos t$, which is the limit of Eqs. (9) and (13) for $\omega\to 0$, yields the same results for the volume fraction and the magnetic dipole moment, but no value for the Brownian relaxation time.

A possible explanation of the increase of the Brownian relaxation time with decreasing frequency might be particle aggregation (dimers, trimers). Those aggregates behave like large particles with a large τ_B. They might be broken up at higher driving frequencies due to the shearing forces. Another explanation is connected with the surfactant layer around the magnetite. Presumably that layer does not have a sharp outer boundary. Due to hydration there will be a continuous transition to the pure carrier fluid (water). The size of that layer might be reduced because of the larger shearing forces at higher frequencies.

The values of $\tau_{B,\mathrm{fit}}$ can be described by a law

$$\frac{1}{\tau_{B,\mathrm{fit}}(f)}=\frac{1}{\tau_{B,0}}+5.6f. \tag{16}$$

The corresponding curve is shown as a solid line. The fit yields $\tau_{B,0}=3.7\times10^{-4}$ s. It can be interpreted as the Brownian relaxation time in the limit of zero frequency of the magnetic field, i.e., in the limit where we assume that the size of the hydration layer is maximal. We cannot provide any explanation for the fitted value 5.6 of the slope of this curve.

The value of $\tau_{B,\mathrm{sus}}$ determined from the measurement of the complex magnetic ac susceptibility is in the same order of magnitude as the values of $\tau_{B,\mathrm{fit}}$.

The results for the hydrodynamic effective volume fraction $\phi_{h,\mathrm{fit}}$ increase first drastically with the driving frequency, but are approximately constant for frequencies larger than 5 kHz. The values seem rather large in comparison to the value $\phi_{\mathrm{random,max}}=0.64$ of the largest possible volume fraction of randomized ordered hard spheres.

In order to further evaluate these values, we estimate in the following the volume fraction using alternative procedures. In accordance with literature there exist different types of volume fractions, namely, the volume fraction of the magnetic active material ϕ_m, the volume fraction of the bare particles ϕ_{core}, and the hydrodynamic effective volume fraction ϕ_h. They follow the relation $\phi_m<\phi_{\mathrm{core}}<\phi_h$, i.e., the volume fractions ϕ_m and ϕ_{core} provide lower bounds for ϕ_h.

The equation

$$\phi_m=\frac{M_s}{M_d} \tag{17}$$

estimates the volume fraction ϕ_m of the magnetic active material in the fluid. In the case of our magnetic fluid one yields $\phi_m=0.036$ with the values provided in Sec. II.

The volume fraction $\phi_{\mathrm{core}}=nV_{\mathrm{core}}$ of the bare particles (n is the number of particles per volume) has to be higher, because the saturation magnetization of small particles is known to be approximately up to 20% smaller than the domain magnetization of the same material [14]. Next we estimate ϕ_{core} from the density of the ferrofluid ρ_{MF}. It is determined primarily by the density of water $\rho_{\mathrm{H_2O}}$ and the

density of magnetite $\rho_{\text{magnetite}}=5.18\times10^3$ kg/m^3. We assume that the volume of the constituents is conserved under mixing:

$$\rho_{\text{magnetite}}\phi_{\text{core}}+\rho_{H_2O}(1-\phi_{\text{core}})=\rho_{MF},$$

which yields

$$\phi_{\text{core}}=\frac{\rho_{MF}-\rho_{H_2O}}{\rho_{\text{magnetite}}-\rho_{H_2O}}=0.045$$

for the volume fraction ϕ_{core}. This result fullfills the 20% rule mentioned above.

As a third alternative, we try to estimate the effective volume fraction directly from the experimental results of the particle diameter and the effective Brownian relaxation time $\tau_{B,\text{sus}}$. We are using the equation

$$\phi_h=nV_h \tag{18}$$

to determine the hydrodynamic effective volume fraction ϕ_h. We obtain an estimate of the particle density n via the equation $n=M_s/m$ and get a value of $n=1.74\times10^{22}$ m^{-3} using the numbers presented above. V_h is determined by the effective relaxation time measured via the ac susceptibility and using Eq. (2). The product nV_h yields 2.2 as an estimate of the volume fraction. This value is much too large to be of physical relevance. An error calculation for this value yields a resulting error of about 75%, when assuming errors for the saturation magnetization, the estimated effective relaxation time, the domain magnetization, and the mean diameter of 5%, 20%, 20%, and 10%, respectively. We believe that the unphysical value reflects the difficulties of the interpretation of V_h in a nondilute suspension, where particle interaction cannot be neglected. Similar difficulties with quantitative comparisons for suspensions with a concentration similar to the one used by us arose even for the case of static magnetic fields [15].

The values for the magnetic dipole moment show a behavior similar to the results for the effective hydrodynamic volume fraction. They first increase drastically with the driving frequency but seem to saturate for frequencies larger than 8 kHz. The results of the fit for the magnetic dipole m are in the same order of magnitude as the value $m=1.1\times10^{-24}$ V s m, as calculated in Sec. II. More precisely for frequencies above 2 kHz the values for the magnetic dipole moment from our fit are about one half larger than this measured value, which yields a factor of $\sqrt[3]{1.5}=1.1$ in the resulting diameter of the bare particles compared to the measured diameter.

For the interpretation of the different values of the three fitting parameters, namely, the Brownian relaxation time, the magnetic dipole moment, and the hydrodynamic effective volume fraction, one has to keep in mind that they are not orthogonal. As a consequence their values tend to influence each other during the fitting procedure.

C. Qualitative comparison — isolines of the reduced viscosity

In the following we compare the contour plot for the experimental results as shown in Fig. 5(a) with the theoretical one in Fig. 5(b). In Fig. 5(a) the isolines of the measured

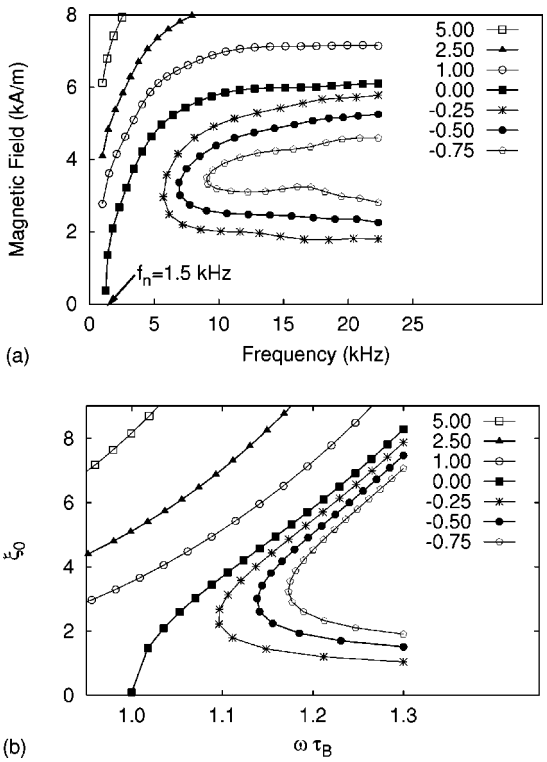

FIG. 5. (a) Contour lines for the reduced viscosity $100\,\eta_r$ in the plane spanned by amplitude and frequency of the magnetic field. (b) Reduced viscosity $\eta_r(H,f)=g\times\frac{3}{2}\phi\times100$, with $\phi=0.2$ determined by numerical integration of the differential equations given in Ref. [10].

reduced viscosity in dependence on the amplitude (ordinate) and on the frequency (abscissa) of the external magnetic field are shown. In Fig. 5(b) the equivalent isolines of the calculated reduced viscosity are plotted, assuming a volume fraction $\phi_h=0.2$. The axes are the amplitude and the circle frequency of the nondimensional magnetic field multiplied by the Brownian relaxation time. In both plots the same symbols denote the same level of the reduced viscosity.

Both contour plots are in good qualitative agreement. They both show a neutral line ($\eta_r=0$) marked by full squares. This line is starting at the abscissa and bending to higher frequencies. Right and below this line in both plots a range of negative viscosity is located, whereas left and above the line an area of positive viscosity is situated. However, both plots do not agree quantitatively. Obviously the curvature of the corresponding isolines differs. In addition the distance between neighboring isolines varies. Thus the frequency axis and the axis for $\omega\tau_B$ cannot be mapped on to each other by a linear transformation.

A quantitative prediction of the models proposed in [9,10] is given by the equation

$$\frac{1}{2\pi f_n}=\tau_B \tag{19}$$

derived for the point f_n where the neutral line meets the frequency axis. We use this relation as an alternative way to determine a value for the Brownian relaxation time

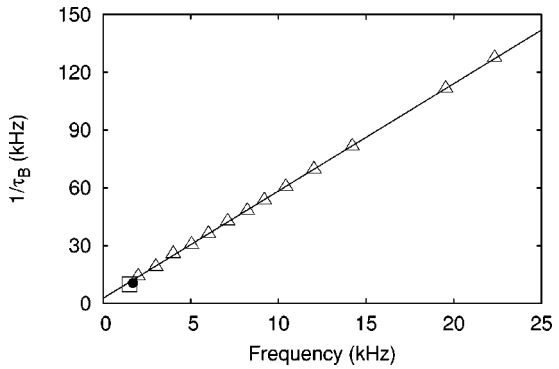

FIG. 6. The inverse of the Brownian relaxation time versus the driving frequency. The open triangles denote $\tau_{B,\mathrm{fit}}$, the solid circle denotes $\tau_{B,\mathrm{sus}}$, and the open square marks $\tau_{B,n}$. The solid line is the fit according to Eq. (16).

$$\tau_{B,n}=\frac{1}{2\pi f_n}\approx 10^{-4}\ \ \mathrm{s},$$

using the frequency $f_n\approx 1500$ Hz from Fig. 5(a).

In order to provide an overview on the different relaxation times measured in this paper, we have plotted in Fig. 6 the inverse of the Brownian relaxation time versus the frequency where they have been obtained. The open triangles correspond to $\tau_{B,\mathrm{fit}}$ as obtained by the fitting procedure. The solid line corresponds to the fit already presented in Fig. 4. Its intersection with the ordinate defines the value of $1/\tau_{B,0}$. This value determines the location on the x axis. The open square marks $\tau_{B,n}$, which has been obtained at a frequency of $f_n=1500$ Hz. $\tau_{B,\mathrm{sus}}$ is displayed by a solid circle. It is determined via $\tau_{B,\mathrm{sus}}=1/(2\pi f_{\max})$, where $f_{\max}$ is the frequency at which the imaginary part of the ac susceptibility is maximal. $f_{\max}$ has been measured to be 1700 Hz. We consider it as extremely remarkable that the value obtained with such a different method agrees reasonably well with the data obtained via the examination of the magnetoviscosity at this frequency. We conclude that the frequency dependence of the Brownian relaxation, as obtained by the fits of the magnetoviscosity, time is of physical origin.

Finally, Table I displays the five values of the Brownian relaxation time determined by the different procedures described in the text.

D. Discussion

Our data can be considered to be in qualitative agreement with the theoretical predictions, but the quantitative comparison reveals two unexpected features: The first intriguing observation is values of the hydrodynamic effective volume fraction which seem to be much too high. That value is, however, extremely hard to interpret in a nondilute suspension. The most remarkable fact is the frequency dependence of the effective Brownian relaxation time. Two reasons can be found why the Brownian relaxation time would be frequency dependent.

(i) We have argued that the thickness of the surfactant layer might be frequency dependent. However, with increasing layer thickness the volume fraction should also increase. The opposite was observed in the results of the fit. Thus this cannot be the full explanation, although it must be kept in mind that the fitting parameters are not orthogonal. In spite of these difficulties it is worth stressing the fact that the Brownian relaxation time obtained via the viscosity measurement coincides with the one obtained via the measurement of the ac susceptibility.

TABLE I. Determined Brownian relaxation times.

Method	Value (s)
$\tau_{B,\mathrm{core}}$	1.5×10^{-6}
$\tau_{B,\mathrm{fit}}$	7.8×10^{-6}–7.1×10^{-5}
$\tau_{B,n}$	1.0×10^{-4}
$\tau_{B,\mathrm{sus}}$	9.4×10^{-5}
$\tau_{B,0}$	3.7×10^{-4}

(ii) A second reason for the frequency dependence can be the formation and destruction of aggregates of particles in the fluid. The theory in [10] was only developed for a dilute dispersion, where chain formation is not important. In this connection it seems worthwhile to point out that the first and only measurement of the negative viscosity effect was performed with a high volume fraction ϕ_{core} of about 20% [10] in order to observe the relatively marginal effect at all. To make closer contact with the theoretical assumptions, we have reduced the volume fraction of the bare particles to $\phi_{\mathrm{core}}=0.045$ and still resolve a negative viscosity of maximal 1%. However, our volume fraction ϕ_{core} could still be too large in order to satisfy the assumptions of the static as well as the dynamic theory.

For the quantitative interpretation of all the fitting parameters it must be kept in mind that the applicability of the theory to our experiment is questionable for two reasons.

(i) The experiment deals with a broad distribution of the particle size and therefore as well distributions of the magnetic moment and the Brownian relaxation time. In contrast the theory assumes particles which are monodisperse.

(ii) In addition, the situation becomes more complicated because the negative viscosity effect has been predicted for ideal nanomotors only, i.e., for $\tau_N/\tau_B\gg 1$. In our case, however, it is not clear whether the Néel relaxation can be neglected completely because of the broad distribution of the particle size.

Considering these two discrepancies it is remarkable that despite the complexity of the experimental situation all qualitative features predicted by the model, including the negative viscosity effect, can be observed in the experiment.

V. CONCLUSION

We have presented a quantitative comparison of a measurement of the negative viscosity effect of a ferrofluid with the theoretical model. Moreover we performed a measurement of the negative viscosity effect of a ferrofluid based on magnetite.

We find a reasonable qualitative agreement between our measurements and the theory given in Ref. [10] for the magnetoviscosity. However, a complete quantitative agreement could not be found. The quantitative comparison unveils two unexpected features. First the fitting procedure yields values

for the volume fraction which seem unrealistic. Second we find a frequency dependence of the parameters of the magnetic fluid, namely, the Brownian relaxation time, the magnetic dipole moment, and the volume fraction. Possible reasons are the variation of the thickness of the surface layer, the existence of aggregates of particles, the distribution of the particle size, and the possible influence of the Néel relaxation. All these complications have not been included in the model. Nevertheless the theoretical model shows all qualitative features of our experiment.

ACKNOWLEDGMENTS

The authors would like to thank Peter Veit for kindly preparing transmission electron microscope pictures of the magnetic particles. They are also grateful to M. Bänitz, M. Justiz, and R. Kötitz for providing them with the opportunity to measure the complex susceptibility. Clarifying discussions with J. Bläsing and M. I. Shliomis are gratefully acknowledged. The experiments were supported by the ''Deutsche Forschungsgemeinschaft'' through Grant No. Re588/10.

[1] A. Einstein, Ann. Phys. (Leipzig) **19**, 289 (1906).
[2] R. E. Rosensweig, *Ferrohydrodynamics* (Cambridge University Press, Cambridge, England, 1985).
[3] R. E. Rosensweig, Science **271**, 614 (1996).
[4] G. Reusing and A. Thomä, Phys. Bl. **52**, 1140 (1996).
[5] Proceedings of the Seventh International Conference on Magnetic Fluids, Bhavnagar, 1995 [J. Magn. Magn. Mater. **149**, 1 (1995)].
[6] J. P. McTague, J. Chem. Phys. **51**, 133 (1969).
[7] M. I. Shliomis, Zh. Eksp. Teor. Fiz. **61**, 2411 (1972) [Sov. Phys. JETP **34**, 1291 (1972)].
[8] M. I. Shliomis, T. P. Lyubimova, and D. V. Lyubimov, Chem. Eng. Commun. **67**, 275 (1988).
[9] M. I. Shliomis and K. I. Morozov, Phys. Fluids **6**, 2855 (1994).
[10] J. C. Bacri, R. Perzynski, M. I. Shliomis, and G. I. Burde, Phys. Rev. Lett. **75**, 2128 (1995).
[11] P. C. Fannin, B. K. P. Scaife, and S. W. Charles, J. Magn. Magn. Mater. **72**, 95 (1988).
[12] M. I. Shliomis, Usp. Fiz. Nauk **112**, 427 (1974) [Sov. Phys. Usp. **112**, 153 (1974)].
[13] W. H. Press, S. A. Teukolsky, W. T. Vetterling, and B. P. Flannery, *Numerical Recipes in FORTRAN*, 2nd ed. (Cambridge University Press, Cambridge, England, 1992).
[14] B. Berkovski and V. Bashtovoy, *Magnetic Fluids and Applications Handbook*, 1st ed. (Begell House, Inc., New York, 1996).
[15] T. Weser and K. Stierstadt, Z. Phys. B **59**, 257 (1985).